AMERICAN SOCIETY FOR MICROBIOLOGY | Journal of Virology®

PATHOGENESIS AND IMMUNITY

Resistance To Poxvirus Lethality Does Not Require the Necroptosis Proteins RIPK3 or MLKL

Brian Montoya,[a] Cory J. Knudson,[a] Carolina R. Melo-Silva,[a] Lingjuan Tang,[a] Samita Kafle,[a] Luis J. Sigal[a]

[a]Department of Microbiology and Immunology, Bluemle Life Science Building, Thomas Jefferson University, Philadelphia, Pennsylvania, USA

ABSTRACT Receptor-interacting protein kinase 3 (RIPK3) and mixed lineage kinase domain-like pseudokinase (MLKL) are proteins that are critical for necroptosis, a mechanism of programmed cell death that is both activated when apoptosis is inhibited and thought to be antiviral. Here, we investigated the role of RIPK3 and MLKL in controlling the Orthopoxvirus ectromelia virus (ECTV), a natural pathogen of the mouse. We found that C57BL/6 (B6) mice deficient in RIPK3 (*Ripk3*$^{-/-}$) or MLKL (*Mlkl*$^{-/-}$) were as susceptible as wild-type (WT) B6 mice to ECTV lethality after low-dose intraperitoneal infection and were as resistant as WT B6 mice after ECTV infection through the natural footpad route. Additionally, after footpad infection, *Mlkl*$^{-/-}$ mice, but not *Ripk3*$^{-/-}$ mice, endured lower viral titers than WT mice in the draining lymph node (dLN) at three days postinfection and in the spleen or in the liver at seven days postinfection. Despite the improved viral control, *Mlkl*$^{-/-}$ mice did not differ from WT mice in the expression of interferons or interferon-stimulated genes or in the recruitment of natural killer (NK) cells and inflammatory monocytes (iMOs) to the dLN. Additionally, the CD8 T-cell responses in *Mlkl*$^{-/-}$ and WT mice were similar, even though in the dLNs of *Mlkl*$^{-/-}$ mice, professional antigen-presenting cells were more heavily infected. Finally, the histopathology in the livers of *Mlkl*$^{-/-}$ and WT mice at 7 dpi did not differ. Thus, the mechanism of the increased virus control by *Mlkl*$^{-/-}$ mice remains to be defined.

IMPORTANCE The molecules RIPK3 and MLKL are required for necroptotic cell death, which is widely thought of as an antiviral mechanism. Here we show that C57BL/6 (B6) mice deficient in RIPK3 or MLKL are as susceptible as WT B6 mice to ECTV lethality after a low-dose intraperitoneal infection and are as resistant as WT B6 mice after ECTV infection through the natural footpad route. Mice deficient in MLKL are more efficient than WT mice at controlling virus loads in various organs. This improved viral control is not due to enhanced interferon, natural killer cell, or CD8 T-cell responses. Overall, the data indicate that deficiencies in the molecules that are critical to necroptosis do not necessarily result in worse outcomes following viral infection and may improve virus control.

KEYWORDS MLKL, RIPK3, ectromelia virus, mice, poxvirus

The receptor-interacting protein kinase 3 (RIPK3) and mixed lineage kinase domain-like pseudokinase (MLKL) proteins are critical for necroptosis, a mechanism of programmed cell death and an alternative to apoptosis (1). When apoptosis is inhibited, viral infection activates necroptosis, which causes the breakdown of the plasma membrane and the release of damage-associated molecular patterns (DAMP) that trigger innate immune responses. Thus, necroptosis is different from apoptosis, which causes blebbing of the plasma membrane and is immunologically silent (2). Of note, RIPK3 is not only important for necroptosis but also plays an important role in (PANoptosis [a process that combines key futures of apoptosis, necroptosis and pyroptosis]) and in some forms of caspase-8-dependent apoptosis and inflammation (3–8). Similarly, MLKL has been shown

Editor Jae U. Jung, Lerner Research Institute, Cleveland Clinic

Address correspondence to Luis J. Sigal, Luis.Sigal@Jefferson.edu.

The authors declare no conflict of interest.

Received 16 December 2022
Accepted 19 December 2022
Published 18 January 2023

to participate in the formation of the NOD^{-}, LRR^{-} and pyrin domain-containing protein 3 (NLRP3) inflammasome downstream of toll-like receptor 3 (TLR3) (9–11).

It is widely thought that necroptosis helps control viral infections by causing the deaths of virus-infected cells and the release of immunogenic damage associated molecular patterns (DAMPs). Supporting the concept that necroptosis is antiviral, intraperitoneal (ip) infection of mice with 2×10^6 plaque-forming units (PFU) of the poorly pathogenic Orthopoxvirus (OPV) vaccinia virus (VACV, the smallpox vaccine) resulted in relatively low virus loads in multiple organs and only 20% death in wild-type (WT) C57BL/6 (B6) mice. However, it caused significantly higher virus loads and 100% lethality to B6 mice deficient in RIPK3 (*Ripk3*$^{-/-}$) (12). This is in spite of VACV and most other OPVs, including the mouse-specific and highly pathogenic OPV ectromelia virus (ECTV), encoding proteins that inhibit apoptosis, such as the inhibitor of caspase-1 and caspase-8 SPI-2 and the Z-RNA-binding protein E3, which competes with the pathogen recognition receptor (PRR) Z-DNA protein binding 1 (ZBP1) for the binding of viral Z-DNA to inhibit ZBP1-mediated RIPK3 activation (13–15). Consistent with the view that necroptosis is antiviral, 60% of *Ripk3*$^{-/-}$ mice, but only 25% of WT mice, succumbed to intranasal infection with 4,000 50% egg infective doses (EID50) of influenza A virus Puerto Rico/8/1934 (IAV PR8) (16). However, in a separate study, 40% of *Mlkl*$^{-/-}$ mice and 100% of WT mice or *Ripk3*$^{-/-}$ mice succumbed to a higher dose of IAV PR8 (6,000 EID50) (17). The improved survival of *Mlkl*$^{-/-}$ mice to the high dose of IAV PR8 was attributed to the decreased recruitment of pathogenic neutrophils to the lungs, which was possibly due to a decreased DAMP release and not to improved virus control (17).

ECTV, the agent of mousepox, is an OPV that naturally infects mice through microabrasions of the footpad (18). Experimentally, at approximately 1 day postinfection (dpi) in the footpad, ECTV spreads to the popliteal draining lymph node (dLN) within infected dendritic cells of the skin (sDC) and replicates in the dLN. At approximately 3 dpi, ECTV spreads lymphohematogenously to the liver and spleen, most likely within infected cells. Mice of mousepox-susceptible strains, such as BALB/c, succumb to fulminant hepatitis at 7 to 13 dpi without an adaptive immune response. In mice of mousepox-resistant strains, such as B6, a strong innate immune response in the dLN restricts the lymphohematogenous spread of ECTV. Consequently, B6 mice have time to mount strong T-cell and antibody responses and thus survive the infection with almost no signs of disease (19).

The protective innate immune response in the dLN of B6 mice is highly orchestrated. Infected sDCs produce the chemokines CCL2 and CCL7, which recruit inflammatory monocytes (iMOs) from the blood to the dLN. When these iMOs become infected (Inf iMO), they produce Type I interferon (IFN-I) via the cGAS-STING-IRF7/NF-κB pathways. IFN-I binds to the interferon alpha receptor (IFNAR) to induce many interferon-stimulated genes (ISG), which are thought to modulate the immune response and play a critical role in curbing the lymphohematogenous spread of ECTV. In addition to recruiting iMOs, sDCs in the dLN also upregulate the expression of NKG2D ligands to induce IFN-gamma (IFN-γ) production in immature, LN-resident natural killer (NK) cells. In response to the IFN-γ, uninfected (bystander) iMOs (Bys iMOs) produce CXCL9, which recruits large numbers of mature NK cells from the blood to the dLN. These newly recruited NK cells produce copious IFN-γ and kill infected cells that downregulate Qa-1^{b} expression, thereby playing a major role in curbing the lymphohematogenous spread of ECTV (20–27).

During viral infections, professional antigen-presenting cells (pAPC) in the dLN, such as dendritic cells (DC), monocytes (MO), and macrophages (Mϕ), become infected or acquire exogenous viral proteins through the phagocytosis of cellular debris and infected cells. As viral proteins are degraded, some resulting peptides bind to major histocompatibility complex I (MHC-I) and are presented at the cell surface. CD8 T-cells recognizing these MHC-I-peptide complexes through their T-cell receptor (TCR), proliferate and differentiate into

effector cytotoxic T Lymphocytes (CTLs) that help control the infection (28). CD8 CTLs are crucial for the resistance of B6 mice to mousepox (29, 30).

WT B6 mice resist footpad ECTV infection, but B6 mice that are deficient in multiple genes that are important for innate or adaptive immunity are highly susceptible. These include, among many others, genes involved in the interferon or NF-κB pathways, such as *Tlr9*, Myd88, *Cgas*, *Sting1*, *Irf7*, *Ifnar1*, *Ifng*, *Ifngr*, and *Nfkb1*. Of note, for all of these genes and pathways, ECTV and other OPVs encode antagonists, most of which are critical for virulence (21, 22, 24–27, 31). Thus, gene targeted B6 mice can be used as a gauge to understand the roles of specific molecules in antiviral resistance, even when the targeted molecules are antagonized by viral immunomodulators. To understand the role of RIPK3 and MLKL in the natural resistance of B6 mice to lethal mousepox, we used *Ripk3*$^{-/-}$ and *Mlkl*$^{-/-}$ mice in a B6 background. Unlike with VACV, *Ripk3*$^{-/-}$ and *Mlkl*$^{-/-}$ mice did not differ from WT mice in their high susceptibility to lethality following low-dose ip ECTV infection. Also similar to WT mice, Ripk3$^{-/-}$ and *Mlkl*$^{-/-}$ mice were fully resistant to lethal mousepox after footpad inoculation. Notably, compared to WT mice, *Mlkl*$^{-/-}$ mice, but not *Ripk3*$^{-/-}$ mice, had lower virus loads in the dLN, spleen, and liver. These data indicated that MLKL deficiency, but not RIPK3 deficiency, improves rather than decreases ECTV control following ECTV infection. Additional experiments indicate that this enhanced ECTV control is not due to increased IFN-I production or improved NK cell or CD8 T-cell responses.

RESULTS

Resistance to peripheral ECTV infection does not require RIPK3 or MLKL. Different from VACV, which is not highly pathogenic in WT mice, ECTV is highly lethal in B6 mice when inoculated ip, even at low doses. To determine the effect of RIPK3 or MLKL deficiency in resistance to ip ECTV, we infected *Ripk3*$^{-/-}$ ($n = 9$), *Mlkl*$^{-/-}$ ($n = 16$), or control WT B6 ($n = 20$) and IFNAR1 deficient (*Ifnar1*$^{-/-}$) ($n = 3$) mice with 10 PFU of ECTV, which is approximately 50% lethal in WT B6 mice. Compared to WT mice (55%), a higher proportion of *Ripk3*$^{-/-}$ (77%) and *Mlkl*$^{-/-}$ (65%) mice succumbed to the infection, though the differences were not statistically significant. As expected, all of the *Ifnar1*$^{-/-}$ mice succumbed to the infection (Fig. 1A). The fact that 55% of the B6 mice succumbed to 10 PFU of ECTV highlights the high pathogenicity of ECTV inoculated ip. This differs from the observation that *Ripk3*$^{-/-}$ mice are more susceptible than WT mice to high-dose ip infection with the OPV VACV (12).

Survival to VACV requires ip inoculation because it is not highly pathogenic to mice. On the other hand, ECTV is a natural mouse pathogen, which, in some mouse strains, such as BALB/c, can cause high lethality when inoculated via its natural route, namely, the footpad. B6 mice are intrinsically resistant to ECTV lethality when infected in the footpad but not when infected ip. However, when B6 mice are deficient in key genes that are necessary for intrinsic ECTV resistance, such as *Myd88*, *Tlr9*, *Ifnar1*, *Nfkb1*, *Irf7*, *cGas*, *Klrd1*, *H2-T23*, and others (20–22, 24–27, 31) they succumb to footpad ECTV infection. Hence, to test the role of RIPK3 and MLKL in the intrinsic resistance to an ECTV infection entering through its natural route, we infected *Ripk3*$^{-/-}$, *Mlkl*$^{-/-}$, and control resistant B6 or susceptible *Tlr9*$^{-/-}$ mice with 3,000 PFU of ECTV in the footpad. As expected, all *Tlr9*$^{-/-}$ mice succumbed to the infection, and all B6 mice resisted the infection. Surprisingly, all *Mlkl*$^{-/-}$ and *Ripk3*$^{-/-}$ mice survived (Fig. 1B) without major signs of disease. Notably, at 7 dpi, the virus titers in the spleens (Fig. 1B) and livers (Fig. 1C) of *Mlkl*$^{-/-}$ mice, but not *Ripk3*$^{-/-}$ mice, were significantly lower than those observed in B6 mice. We also analyzed virus titers in the dLN at 3 dpi, when the innate immune response peaks in the dLN and controls the spread of ECTV to the spleen and liver (26). The results showed that *Mlkl*$^{-/-}$ mice, but not *Ripk3*$^{-/-}$ mice, had significantly lower virus loads in the dLN than WT B6 mice (Fig. 1D). These unexpected results indicated that, (i) different from several other key innate immune molecules, such as NFKB1, TLR9, MyD88, etc., RIPK3 and MLKL are not necessary for the intrinsic resistance of B6 mice to ECTV infection after footpad inoculation and that (ii) a deficiency in MLKL, which participates in necroptosis, but not in RIPK3, which participates in necroptosis,

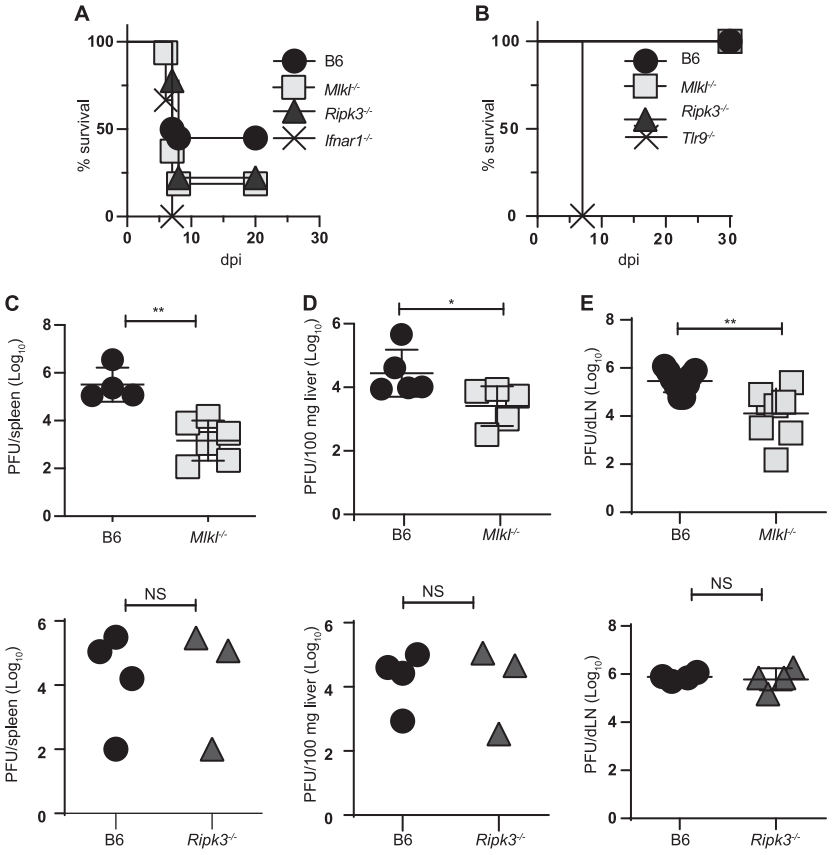

FIG 1 Necroptosis deficiency improves ECTV control. (A) B6 (n = 20), *Ripk3*$^{-/-}$ (n = 9), *Mlkl*$^{-/-}$ (n = 16), and *Ifnar1*$^{-/-}$ (n = 3) mice were infected ip with 10 PFU ECTV and were observed for survival. The data correspond to 5 to 8 mice per group and represent two combined experiments. (B) B6, *Tlr9*$^{-/-}$, and *Mlkl*$^{-/-}$ mice were infected in the footpad with 3,000 PFU ECTV and observed for survival. The data correspond to 5 mice per group and represent two independent experiments. (C–E) Virus titers were determined via plaque assay in the spleen (C) and liver (D) at 7 dpi and in the dLN at 3 dpi (E). The data correspond to 4 to 6 mice per group and represent two independent experiments. The data in panels C–E were analyzed with a nonparametric Mann-Whitney test using Prism software. *, $P < 0.05$; **, $P < 0.01$.

apoptosis, PANoptosis, and other mechanisms of inflammation (10, 32), increases ECTV control after footpad inoculation.

***Mlkl*$^{-/-}$ mice do not have increased expression of IFN or ISG in the dLN.** The reduced ECTV loads in the dLN of *Mlkl*$^{-/-}$ mice at 3 dpi suggested that an enhanced IFN response in the dLN could be at least partly responsible for the increased control of ECTV after footpad infection.

IFN-I in the dLN is mainly produced by infected iMOs (27) and is critical to curbing ECTV replication and its spread to the liver and the spleen (24, 26, 27). In addition, NK cells recruited to the dLN produce IFN-γ, which is also critical to curbing the systemic dissemination of ECTV (33).

We hypothesized that MLKL deficiency could result in the increased expression of transcripts for IFN-I, IFN-γ, or interferon-stimulated genes (ISG) in the dLN. Nevertheless, at 3 dpi, the dLNs of WT B6, *Ripk3*$^{-/-}$,or *Mlkl*$^{-/-}$ mice had no statistically significant differences in their expression of transcripts for the IFN-I genes *Ifnb1*, *Ifna2*, *Ifna4*, *Ifna5*, and *non-4 Ifna* (using common primers for all of the *Ifna* genes, except for *Ifna4*) (Fig. 2A), for *Ifng* (Fig. 2B) or for the ISGs *Ifit3*, *Irf7*, *Sting1*, and *Isg15* (Fig. 2C). Thus, enhanced IFN expression or signaling was not responsible for the increased control of ECTV in MLKL deficient mice. Because differences in titers were observed in *Mlkl*$^{-/-}$ mice, but not in *Ripk3*$^{-/-}$ mice, we focused on these mice for the remainder of our study.

***Mlkl*$^{-/-}$ mice do not have increased NK cell responses in the dLN.** NK cells are recruited from the blood to the dLN at 2 to 3 dpi and play a crucial role in restricting

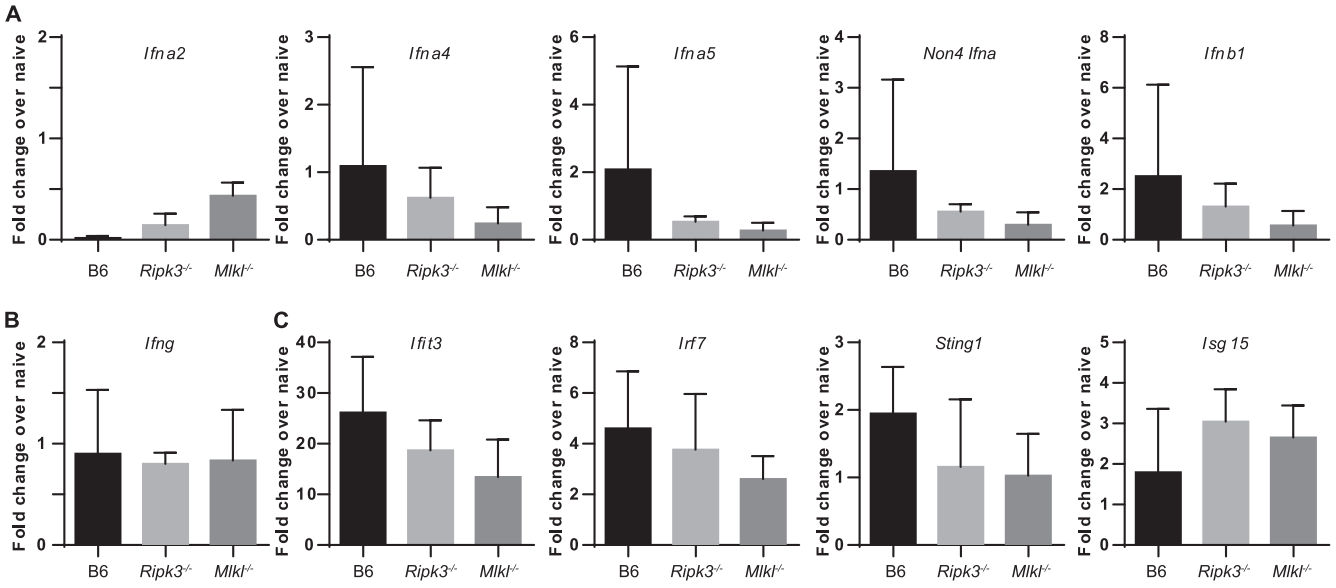

FIG 2 *Mlkl*$^{-/-}$ mice do not have increased expression of IFN or ISG in the dLN. B6 and *Mlkl*$^{-/-}$ mice were infected with 3,000 PFU ECTV in the footpad. Their dLNs were collected and analyzed via quantitative reverse transcriptase PCR at 3 dpi. (A) Expression of the indicated IFN-I transcripts. (B) Expression of IFN-γ transcripts. (C) Expression of the indicated ISGs. The data represent the mean ± SEM of three mice/group and are representative of two independent experiments. The data were analyzed with a Mann-Whitney test using Prism software. The comparisons were not statistically significant.

the dissemination of ECTV to the liver and spleen. We hypothesized that a stronger NK cell response in the dLNs of *Mlkl*$^{-/-}$ mice could play a role in their increased resistance to ECTV infection. However, at 3 dpi, the dLN of *Mlkl*$^{-/-}$ and WT B6 mice did not differ in the frequency (Fig. 3A and B) or total number (Fig. 3A and C) of NK cells or in their production of IFN-γ (Fig. 3A and D). Hence, enhanced NK cell responses in the dLN were not responsible for the increased control of ECTV in MLKL-deficient mice.

***Mlkl*$^{-/-}$ mice have increased numbers of infected APC presenting antigenic peptides on MHC-I.** DCs, iMOs, and B-lymphocytes are the main targets of ECTV infection in the dLN. Furthermore, iMOs and DCs are well-known pAPCs for CD8 T-cells (28). We hypothesized that ECTV-infected *Mlkl*$^{-/-}$ cells could survive longer than their WT counterparts, thereby extending their ability to present antigenic peptides on MHC-I. To test for this possibility, we infected B6 and *Mlkl*$^{-/-}$ mice with ECTV-OVA-GFP (31), a recombinant ECTV virus coexpressing green fluorescence protein (GFP) and chicken ovalbumin (OVA). Using this virus, infected B-lymphocytes, iMOs, and DCs can be identified as GFP$^+$, and those presenting the immunodominant CD8 T-cell OVA epitope SIINFEKL bound to the MHC-I molecule H2-K^b (K^b) can be recognized via staining with the monoclonal antibody (MAb) 25-D1.16, which is specific for K^b-SIINFEKL complexes (34).

At 3 dpi, B6 and *Mlkl*$^{-/-}$ mice did not differ in the absolute numbers of iMOs, DCs, or B-lymphocytes in their dLNs. Consistent with the hypothesis that necroptosis deficiency extends the survival of infected cells, the dLNs of *Mlkl*$^{-/-}$ mice had higher frequencies and absolute numbers of infected (GFP$^+$) iMOs, DCs, and B-lymphocytes than the dLNs of WT B6 mice. Moreover, the mean fluorescence intensities (MFI) of the GFP$^+$ iMOs and DCs, but not B lymphocytes, were significantly higher in *Mlkl*$^{-/-}$ mice than in WT B6 mice, suggesting extended viral transcription. Consistently, the frequency and total numbers of 25-D1.16$^+$ iMOs, DCs, and B-lymphocytes were significantly higher in *Mlkl*$^{-/-}$ mice than in WT B6 mice, indicating that in the absence of necroptosis, more infected cells present viral antigens on MHC-I. However, the mean fluorescence intensity for 25-D1.16 staining was similar for WT and *Mlkl*$^{-/-}$ infected cells (Fig. 4A–G), indicating that extended survival does not increase the efficiency of MHC-I antigen presentation. Of note, we did not detect differences in the frequencies of total Zombie-Violet$^+$ (ZV$^+$; an indicator of dead cells) or of GFP$^+$ ZV$^+$ iMO (reported as text), probably because dead cells are rapidly cleared *in vivo*.

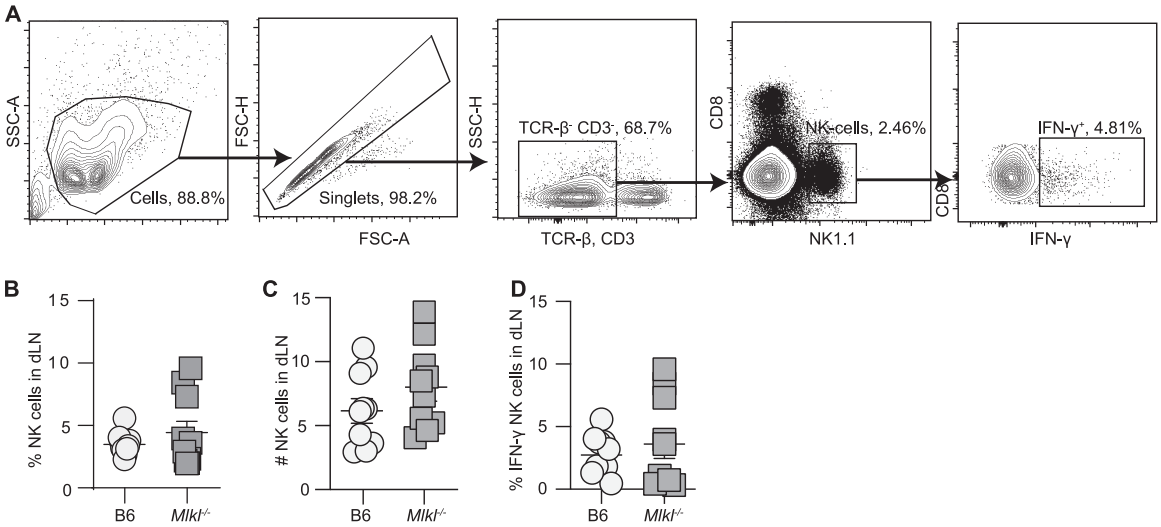

FIG 3 *Mlkl*$^{-/-}$ mice do not have increased NK cell responses in the dLN. B6 and *Mlkl*$^{-/-}$ mice were infected with 3,000 PFU ECTV in the footpad. At 3 dpi, their dLNs were collected and analyzed via flow cytometry. (A) Gating strategy to identify NK cells. (B) Frequency of NK cells. (C) Total number of NK cells. (D) Frequency of IFN-γ producing NK cells. The data correspond to 10 individual mice per group from 2 aggregated experiments. The data were analyzed with a Mann-Whitney test using Prism software. The comparisons were not statistically significant.

***Mlkl*$^{-/-}$ mice do not have increased CD8 T-cell responses.** CD8 T-cells play a fundamental role in controlling the virus titers in the spleen and liver at 6 to 8 dpi with ECTV in the footpad (30, 35). We hypothesized that the increased number of pAPCs presenting antigens could produce more rapid or potent CD8 T-cell responses in *Mlkl*$^{-/-}$ mice. To test for this possibility, we infected B6 and *Mlkl*$^{-/-}$ mice with ECTV and analyzed their CD8 T-cell responses, which peak at 7 to 8 dpi in B6 mice. To determine the total anti-ECTV response, we analyzed CD8 T-cells for the presence of CD44 and granzyme B (GzmB), which we have shown mark virus-specific cells (33). At 6 dpi, the frequencies of CD44^{+} GzmB^{+} CD8 T-cells in the spleens of B6 and *Mlkl*$^{-/-}$ mice were similar and relatively low, but they increased to similarly high levels at 8 dpi (Fig. 5A and B). Consistently, the frequencies and absolute numbers of CD8 T-cells that were specific for the immunodominant, K^{b}-restricted ECTV CD8 T-cell epitope TSYKFESV were still incipient at 6 dpi, and they increased to similarly high levels in the spleens and livers of B6 and *Mlkl*$^{-/-}$ mice at 8 dpi (Fig. 5A and B). Hence, faster or stronger CD8 T-cell responses were not responsible for the enhanced virus control in the spleens and livers of *Mlkl*$^{-/-}$ mice. Finally, to determine the inflammation and liver damage, we performed histopathology of the livers at 7 dpi. We found that the livers of B6 and *Mlkl*$^{-/-}$ mice contained multiple and similarly sized foci of immune cell infiltration, suggesting comparable inflammation. They also lacked necrotic areas, demonstrating protection. This contrasted with the livers of ECTV-susceptible *Tlr9*$^{-/-}$ mice, which did not have foci of immune cell infiltration and had extensive necrotic areas (Fig. 5C).

DISCUSSION

Many viruses produce proteins that antagonize apoptosis or necroptosis (36–38), including herpesviruses and poxviruses (36–38). Moreover, under some experimental conditions, RIPK3 or MLKL deficiency results in decreased virus control (12). Because of this, necroptosis is generally regarded as a programmed mechanism of cell death that is operative when apoptosis is blocked and contributes to virus control (39). Using *Mlkl*$^{-/-}$ and *Ripk3*$^{-/-}$ mice in the mousepox-resistant B6 background, we demonstrate that, unlike with VACV, mice deficient in *Ripk3*$^{-/-}$ or *Mlkl*$^{-/-}$ are as sensitive as WT B6 mice when infected ip with ECTV. However, unlike mousepox-sensitive *Tlr9*$^{-/-}$ mice, but similar to WT mice, *Ripk3*$^{-/-}$ and *Mlkl*$^{-/-}$ mice survived after a footpad ECTV infection. Furthermore, *Mlkl*$^{-/-}$ mice endured lower virus loads than WT mice in the liver

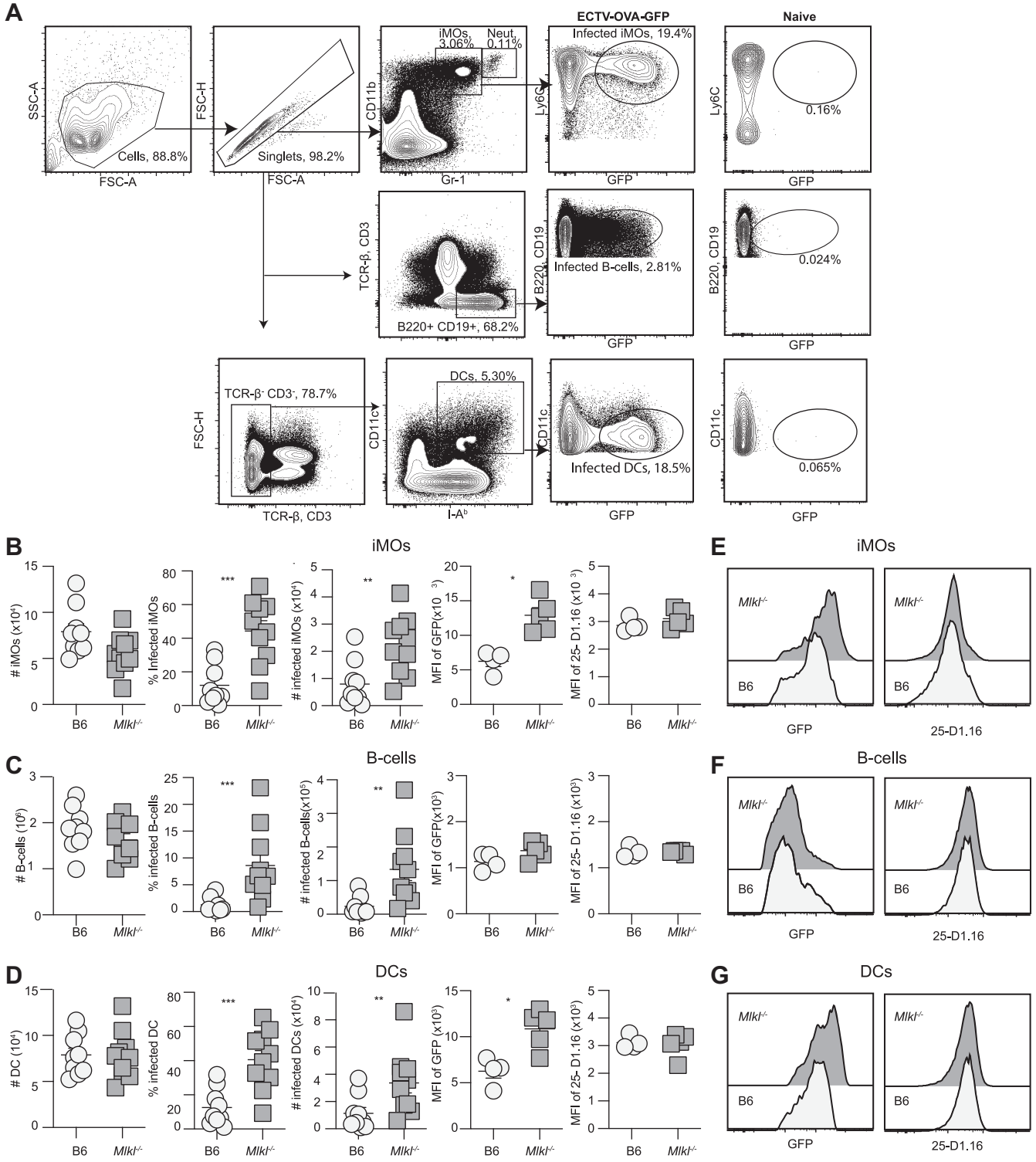

FIG 4 *Mlkl*$^{-/-}$ mice have increased numbers of infected APC presenting antigenic peptides on MHC-I. B6 and *Mlkl*$^{-/-}$ mice were infected in the footpad with 3,000 ECTV-OVA-GFP. At 3 dpi, the dLNs were collected and analyzed via flow cytometry. (A) Gating strategy for analyzing infection and antigen presentation in iMOs, DCs, and B-lymphocytes. Naïve controls are represented to the right of the indicated cell populations. (B–D) The total number, frequency of infected, the total number of infected (GFP^{+}), the MFI of infected, the frequency presenting SIINFEKL (25-D1.16^{+}), the total number presenting SIINFEKL, and the MFI of cells presenting SIINFEKL are shown for the iMOs (B), DCs (C), and B-lymphocytes (D). Representative histograms of *Mlkl*$^{-/-}$ (background, dark gray) and B6 (foreground, light gray) MFIs of GFP and 25-D1.16 from the indicated cell populations (E–G). The data correspond to 10 mice from 2 aggregated experiments. The data correspond to individual mice. The data were analyzed using the Mann-Whitney test with Prism software. *, $P < 0.05$; **, $P < 0.01$; ***, $P < 0.001$. The others were not statistically significant.

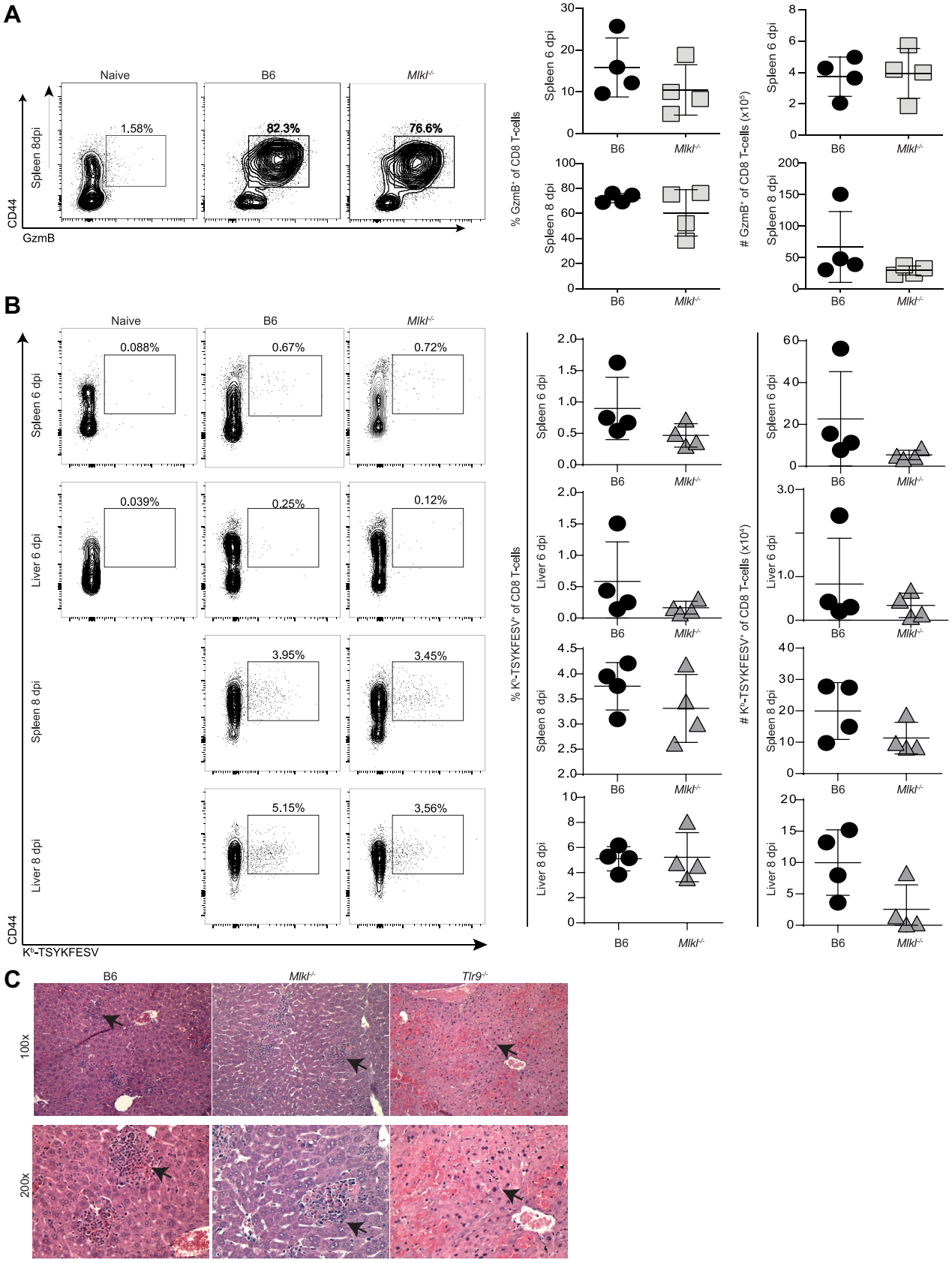

FIG 5 *Mlkl*$^{-/-}$ mice do not have increased CD8 T-cell responses. B6 and *Mlkl*$^{-/-}$ mice were infected in the footpad with 3,000 PFU ECTV. Their spleens and livers were collected at 6 or 8 dpi, and their CD8 T-cell responses were analyzed via flow cytometry. (A) Representative samples (left panel) as well

(Continued on next page)

and the spleen at 7 dpi and in the dLN at 3 dpi. These results indicate that (i) RIPK3 and MLKL deficiencies do not increase susceptibility to a highly pathogenic OPV following unnatural ip inoculation, and (ii) RIPK3 and MLKL are unnecessary when ECTV enters its host through what is considered to be its natural route. Because ECTV encodes proteins that suppress RIPK3 and MLKL activation, it could be argued that the reason that *Ripk3*$^{-/-}$ and *Mlkl*$^{-/-}$ mice survive footpad infection is that the two proteins are no longer functional. However, precedent with many other immune evasion proteins suggests that this might not be the case. For example, mice deficient in *Myd88*, *Cgas*, *Sting*, *Nfkb1*, *Irf7*, or *Ifnar1* are highly sensitive to ECTV footpad infection, although ECTV encodes proteins that block the functions of their products (21, 22, 24, 25, 40–43). Of note, it has been recently argued that RIPK3 is important in the control of OPV because the cowpox virus (CPXV) protein CPXV006 (named by the authors "virus inducer of RIPK3 degradation" or vIRD), promoted RIPK3 degradation, and CPXV deficient in CPXV006 (CPXV-Δ006) was slightly attenuated in WT B6 mice, but regained pathogenicity in *Ripk3*$^{-/-}$ mice when inoculated ip at a high dose of 10^6 PFU (38). Yet, CPXV006 had been previously shown to inhibit NF-κB by promoting NF-κB1/p105 degradation (44). Moreover, the homolog of CPXV006 in ECTV is ECTV002 (45), and we have previously shown that ECTV deficient in EVM002 (ECTV-Δ002) inoculated into the footpad was innocuous in mousepox-susceptible BALB/c mice at 10^5 PFU but was fully lethal to *Nfkb1*$^{-/-}$mice at only 3,000 PFU. Moreover, we have shown that ECTV-Δ002 induced more NF-κB activation and inflammatory cytokines than WT ECTV in BALB/c mice, strongly supporting a role for EVM002 and CPXV006 as NF-κB inhibitors *in vivo* (22).

At 2 to 3 dpi, iMOs and NK cells are recruited to the dLNs of ECTV-infected B6 mice. The iMOs that become infected produce IFN-I, while the NK cells produce IFN-γ and kill infected cells in the dLN. IFN-I and the effector functions of NK cells are critical to controlling the spread of ECTV from the dLN to the liver and spleen in B6 mice (26). To identify the possible mechanisms of improved virus control during necroptosis deficiency, we compared the innate immune responses of B6, *Ripk3*$^{-/-}$ and *Mlkl*$^{-/-}$ mice at 3 dpi. We found that neither MLKL nor RIPK3 deficiency affected IFN-I, IFN-γ, or ISG expression in the dLN, nor did these deficiencies affect the recruitment of IFN-γ producing NK cells or IFN-I producing iMOs to the dLN. However, MLKL deficiency increased the relative and absolute numbers of infected iMOs and DCs that presented antigens on MHC-I. Because it is well-established that DCs and iMOs are pAPC that prime CD8 T-cell responses, and because CD8 T-cells are essential to the control of ECTV at 7 to 8 dpi (46), we tested whether the increased frequency of APCs presenting antigens correlated with increased CD8 T-cell responses. However, the CD8 T-cell responses in *Mlkl*$^{-/-}$ mice were quantitatively and qualitatively similar to those observed in B6 mice. Therefore, the improved virus control in *Mlkl*$^{-/-}$ mice was not due to an increase in the potency of the CD8 T-cell response.

The finding that MLKL deficiency improves virus control, depending on the route of infection, is intriguing and may have important implications for the treatment of viral infections that spread lymphohematogenously. Despite pursuing several promising avenues, we could not identify the mechanism by which MLKL favors ECTV control. It has been shown that RIPK3 may regulate vascular permeability (47). This could also be a function of MLKL. Thus, one hypothesis is that changes in vascular permeability could delay the spread of ECTV from the footpad to the dLN. However, if this hypothesis were correct, it is difficult to understand why MLKL mice, but not RIPK3 mice, would

FIG 5 Legend (Continued)
as the frequency and total number of CD44$^+$ GzmB$^+$ CD8 T cells in the spleens of B6 and *Mlkl*$^{-/-}$ mice at 6 and 8 dpi, as indicated (right panel). The data correspond to four individual mice and are representative of two experiments. (B) Representative samples (left panel) as well as the frequency and the total number of CD44$^+$ TSYKFESV-specific (Kb-TSYKFESV dimer$^+$) CD8 T-cells in the spleens and livers of B6 and *Mlkl*$^{-/-}$ mice at 6 and 8 dpi, as indicated (right panel). (C) Representative histology of B6, *Mlkl*$^{-/-}$, and *Tlr9*$^{-/-}$ livers at 7 dpi. The data correspond to four individual mice per group and represent two independent experiments. The arrows with the livers of the B6 and *Mlkl*$^{-/-}$ mice show areas of leukocyte accumulation, and, in the *Tlr9*$^{-/-}$ mice, areas of necrosis. All of the data were analyzed with a Mann-Whitney test using Prism software. The comparisons were not statistically significant.

have decreased virus loads. Thus, we believe it is more likely that other, yet undiscovered cell-death-independent functions of MLKL are responsible for the enhanced control of ECTV in *Mlkl*$^{-/-}$ mice, following footpad infection.

MATERIALS AND METHODS

Mice. All of the experiments were approved by the Thomas Jefferson University Institutional Animal Care and Use Committee (IACUC). Wild-type C57BL/6N mice were purchased from Charles River. *Mlkl*$^{-/-}$ mice (1) were generously provided by James Murphy (The Walter and Eliza Hall Institute of Medical Research, Parkville, VIC 3052, Australia). All of the mice were bred and maintained in-house. For all of the experiments, the mice were gender-matched and age-matched, and they were between 6 and 12 weeks of age.

Viruses and infection. The ECTV strain Moscow was obtained from ATCC (VR-1374) and propagated as previously described (48). The recombinant ECTV-GFP (31) and ECTV-OVA-GFP (49) were propagated similarly. For all of the experiments, the mice were injected with 3,000 PFU of virus in 30 μL PBS. For the survival experiments, the mice were observed daily for signs of morbidity. The titers of ECTV were determined via plaque assay as previously described (24). Briefly, BS-C-1 cells (ATCC CCL-26) were grown in 24-well tissue culture plates to 80 to 90% confluence in DMEM tissue culture medium (Invitrogen Life Technologies) supplemented with 10% fetal calf serum (FCS; Sigma-Aldrich), 4.5 g/L glucose, 4.5 g/L L-glutamine, 4.5 g/L sodium pyruvate, 1× nonessential amino acids, and 100 IU/mL penicillin and streptomycin (Complete DMEM). BS-C-1 monolayers were infected with 10-fold dilutions of organ homogenate for 1.5 h at 37°C with 5% CO_2 in complete DMEM medium containing 2% FCS. The organ homogenates were made while processing samples for flow cytometry or via whole organ mechanical disruption using a TissueLyser (Qiagen) with a frequency of 30 iterations/second for 2 min. Following incubation, the virus was removed, and the monolayers were overlaid with a 1:1 mixture of 2% carboxymethyl cellulose in complete DMEM medium containing 5% FCS. After 4 to 5 days of incubation at 37°C with 5% CO_2, the monolayers were fixed for 20 min at room temperature in 1% crystal violet in 20% ethanol solution and 4% paraformaldehyde. The excess crystal violet was washed off in a pool of water, and the plaques were quantified.

Cell isolation for flow cytometry. The mice were euthanized by cervical dislocation. The popliteal lymph nodes were incubated in Liberase TM (1.67 Wunsch units/mL) (Sigma) in PBS with 25 mM HEPES for 30 min at 37°C. PBS with 25 mM HEPES + 10% FBS was added to disrupt the digestion process, and the samples were mechanically homogenized via pipetting with 21-gauge needles (BD) and a 1 mL syringe (BD). The samples were filtered through a 70 μm mesh and washed with PBS for flow cytometry analysis.

The spleens were processed into single-cell suspensions via gentle tissue dissociation using frosted microscope slides (Fisher Scientific). The livers were carefully manipulated through a stainless steel wire mesh (88 T316 0.0035-inch diameter; TWC) in a 1.5 × 1.25 in polyvinyl chloride (PVC) female trap adaptor (number 4804; Nibco). Hepatocytes were removed following resuspension in 37% Percoll (GE Healthcare Life Sciences) and centrifugation for 20 min at a relative centrifugal force of 930 at room temperature. The resulting liver cell pellets or splenocytes were treated with ammonium chloride potassium (ACK) buffer (155 mM NH4Cl, 1 mM KHCO3, 0.1 mM EDTA) for 5 min to lyse the red blood cells, washed with RPMI 1640 medium, and then stained with the appropriate antibodies, as described below.

Flow cytometry. The flow cytometry was performed as previously described (23, 24). The following antibodies were used: PE-Ly6c (Clone HK1.4, BioLegend), PerCP/cy5.5-B220 (Clone RA3-6B2, BioLegend), CD19 (Clone 6D5, BioLegend), PeCy7- CD11c (Clone N418, BioLegend), APCfire- Gr-1 (Clone RB6-8C5, BioLegend), Pacific Blue- I-Ab (Clone AF6-120.1, BioLegend), BV605- CD11b (Clone M1/70, BioLegend), BV786- TCRb (Clone H57-597, BD Biosciences), and CD3 (Clone 17A2, BioLegend). 25-D1.16 was conjugated to APC with the molecular probes AlexaFlour 647 carboxylic acid and succinimidyl ester reagent, according to the manufacturers' instructions. To measure the K^b-TSYKFESV-specific responses in the spleen and liver samples, we used the following antibodies: BUV395-CD4 (GK1.5, BD Biosciences), APCfire-CD8 (Clone 53-6.7, BioLegend), BV605-TCRb (Clone H57-597, BioLegend), and AF488- NK1.1 (Clone PK136, BioLegend). BD DimerX K^b (BD Biosciences) molecules were incubated with TSYKFESV peptide and PBS (0.2:0.075:0.725 volume ratio) overnight at 37°C. DimerX K^b-TSYKFESV complexes were conjugated with anti-mouse IgG1 at a volume ratio of 4:1 (clone RMG1-1; PE) for 1 h at room temperature. The cells were incubated with 1 μL DimerX K^b-TSYKFESV-PE complexes for 30 min at 4°C before staining with other extracellular Abs. For intracellular staining, the samples were stained as described above and were then fixed for 10 min in 1% paraformaldehyde in PBS. The cells were then incubated in 1× Perm/Wash buffer (BD Biosciences) for 5 min at 4°C and stained for 30 min with the following Abs in 1× Perm/Wash buffer: Pacific Blue- GzmB (Clone GB11, BioLegend), PeCy7-IFNg (XMG1.2, BioLegend), and PE-K_i-67 (Clone 16-A8, BioLegend). All of the samples were analyzed on a BD Fortessa. The histology was performed on thin, paraffin-embedded sections. Serial sections were stained with hematoxylin and eosin and were imaged using a Leica DM5000 B microscope.

RNA preparation and RT-qPCR. The dLNs of B6 or *Mlkl*$^{-/-}$ mice at 3 dpi were obtained and stored in RNA*later* RNA stabilization reagent at 4°C until RNA isolation. Total RNA was obtained using a Qiagen RNeasy Kit, according to the manufacturer's instructions. The total RNA samples were synthesized into cDNA using a High Capacity cDNA Reverse Transcription Kit (Life Technologies), according to the manufacturer's instructions and as previously described (22). Approximately 1 ng of cDNA from each sample was run in a 20 μL reaction using iTaq2 Universal SYBR Green PCR Mix (Bio-Rad) using a Bio-Rad CFX96. The ratios of the mRNA levels to the control values were calculated using the ΔCt method at a threshold

of 0.02. All of the data were normalized to control GAPDH. The qPCR conditions were as follows: hold for 10 min at 95°C and then 40 cycles of 15 s at 95°C and 60 s at 60°C. The primers used were as follows (forward and reverse, 5′–3′): GAPDH, tgtccgtcgtggatctgac and cctgcttcaccaccttcttg; *Ifnb1*, cacagccctctccatcaacta and catttccgaatgttcgtcct; *Ifna2*, atgaggaggctccccttttc and accttctccaggggggaatc; *Ifna4*, gtcttttgatgtgaagaggttcaa and tcaagccatccttgtgctaa; *Ifna5*, gccttaaccctcctggtaaaa and tcctgtgggaatccaaagtc; *non-4 Ifna*, aagctgtgtgatgcaacaggt and ggaacacagtgatcctgtgg; IFN-*γ*, gcaaaaggatggtgacatga and ttcaagacttcaaagagtctgaggta; *Ifit3*, tgaactgctcagcccaca and tcccggttgacctcactc; *Irf7*, cttcagcactttcttccgaga and tgtagtgtggtgacccttgc; *Sting1*, cagcgtctacgagattctgga and acatggcaaacagggtctg; *Isg15*, agtcgacccagtctctgactct and ccccagcatcttcaccttta.

ACKNOWLEDGMENTS

We thank Jianke Zhang for the provision of *Mlkl*$^{-/-}$ mice and James Murphy for giving permission for their utilization.

This work was supported by grants R56AI110457 and R01AI110457 from NIAID. Grant T32 AI134646 from NIAID supported B.M. The present research utilized the Flow Cytometry and Laboratory Animal facilities at SKCC at Jefferson Health (supported by NCI- P30CA056036).

B.M. and L.J.S. conceived and designed the experiments, analyzed the data and the results, and cowrote the paper. B.M. performed most of the experiments. L.J.S. supervised the work. C.J.K., C.R.M.-S., S.K., and L.T. performed some of the experiments.

We have no competing interests to declare.

REFERENCES

1. Murphy JM, Czabotar PE, Hildebrand JM, Lucet IS, Zhang JG, Alvarez-Diaz S, Lewis R, Lalaoui N, Metcalf D, Webb AI, Young SN, Varghese LN, Tannahill GM, Hatchell EC, Majewski IJ, Okamoto T, Dobson RC, Hilton DJ, Babon JJ, Nicola NA, Strasser A, Silke J, Alexander WS. 2013. The pseudokinase MLKL mediates necroptosis via a molecular switch mechanism. Immunity 39:443–453. https://doi.org/10.1016/j.immuni.2013.06.018.
2. Peltzer N, Walczak H. 2019. Cell death and inflammation - a vital but dangerous liaison. Trends Immunol 40:387–402. https://doi.org/10.1016/j.it.2019.03.006.
3. Christgen S, Zheng M, Kesavardhana S, Karki R, Malireddi RKS, Banoth B, Place DE, Briard B, Sharma BR, Tuladhar S, Samir P, Burton A, Kanneganti TD. 2020. Identification of the PANoptosome: a molecular platform triggering pyroptosis, apoptosis, and necroptosis (PANoptosis). Front Cell Infect Microbiol 10:237. https://doi.org/10.3389/fcimb.2020.00237.
4. Malireddi RKS, Kesavardhana S, Kanneganti TD. 2019. ZBP1 and TAK1: master regulators of NLRP3 inflammasome/pyroptosis, apoptosis, and necroptosis (PAN-optosis). Front Cell Infect Microbiol 9:406. https://doi.org/10.3389/fcimb.2019.00406.
5. Lawlor KE, Khan N, Mildenhall A, Gerlic M, Croker BA, D'Cruz AA, Hall C, Kaur Spall S, Anderton H, Masters SL, Rashidi M, Wicks IP, Alexander WS, Mitsuuchi Y, Benetatos CA, Condon SM, Wong WW, Silke J, Vaux DL, Vince JE. 2015. RIPK3 promotes cell death and NLRP3 inflammasome activation in the absence of MLKL. Nat Commun 6:6282. https://doi.org/10.1038/ncomms7282.
6. Khan N, Lawlor KE, Murphy JM, Vince JE. 2014. More to life than death: molecular determinants of necroptotic and non-necroptotic RIP3 kinase signaling. Curr Opin Immunol 26:76–89. https://doi.org/10.1016/j.coi.2013.10.017.
7. Vince JE, Wong WW, Gentle I, Lawlor KE, Allam R, O'Reilly L, Mason K, Gross O, Ma S, Guarda G, Anderton H, Castillo R, Hacker G, Silke J, Tschopp J. 2012. Inhibitor of apoptosis proteins limit RIP3 kinase-dependent interleukin-1 activation. Immunity 36:215–227. https://doi.org/10.1016/j.immuni.2012.01.012.
8. Newton K, Dugger DL, Wickliffe KE, Kapoor N, de Almagro MC, Vucic D, Komuves L, Ferrando RE, French DM, Webster J, Roose-Girma M, Warming S, Dixit VM. 2014. Activity of protein kinase RIPK3 determines whether cells die by necroptosis or apoptosis. Science 343:1357–1360. https://doi.org/10.1126/science.1249361.
9. Kang S, Fernandes-Alnemri T, Rogers C, Mayes L, Wang Y, Dillon C, Roback L, Kaiser W, Oberst A, Sagara J, Fitzgerald KA, Green DR, Zhang J, Mocarski ES, Alnemri ES. 2015. Caspase-8 scaffolding function and MLKL regulate NLRP3 inflammasome activation downstream of TLR3. Nat Commun 6:7515. https://doi.org/10.1038/ncomms8515.
10. Gullett JM, Tweedell RE, Kanneganti TD. 2022. It's all in the PAN: crosstalk, plasticity, redundancies, switches, and interconnectedness encompassed by PANoptosis underlying the totality of cell death-associated biological effects. Cells 11:1495. https://doi.org/10.3390/cells11091495.
11. Conos SA, Chen KW, De Nardo D, Hara H, Whitehead L, Nunez G, Masters SL, Murphy JM, Schroder K, Vaux DL, Lawlor KE, Lindqvist LM, Vince JE. 2017. Active MLKL triggers the NLRP3 inflammasome in a cell-intrinsic manner. Proc Natl Acad Sci U S A 114:E961–E969.
12. Cho YS, Challa S, Moquin D, Genga R, Ray TD, Guildford M, Chan FK. 2009. Phosphorylation-driven assembly of the RIP1-RIP3 complex regulates programmed necrosis and virus-induced inflammation. Cell 137:1112–1123. https://doi.org/10.1016/j.cell.2009.05.037.
13. Koehler H, Cotsmire S, Zhang T, Balachandran S, Upton JW, Langland J, Kalman D, Jacobs BL, Mocarski ES. 2021. Vaccinia virus E3 prevents sensing of Z-RNA to block ZBP1-dependent necroptosis. Cell Host Microbe 29:1266–1276. https://doi.org/10.1016/j.chom.2021.05.009.
14. Frey TR, Forsyth KS, Sheehan MM, De Haven BC, Pevarnik JG, Hand ES, Pizzorno MC, Eisenlohr LC, Hersperger AR. 2018. Ectromelia virus lacking the E3L ortholog is replication-defective and nonpathogenic but does induce protective immunity in a mouse strain susceptible to lethal mousepox. Virology 518:335–348. https://doi.org/10.1016/j.virol.2018.03.016.
15. Koehler H, Cotsmire S, Langland J, Kibler KV, Kalman D, Upton JW, Mocarski ES, Jacobs BL. 2017. Inhibition of DAI-dependent necroptosis by the Z-DNA binding domain of the vaccinia virus innate immune evasion protein, E3. Proc Natl Acad Sci U S A 114:11506–11511. https://doi.org/10.1073/pnas.1700999114.
16. Nogusa S, Thapa RJ, Dillon CP, Liedmann S, Oguin TH, 3rd, Ingram JP, Rodriguez DA, Kosoff R, Sharma S, Sturm O, Verbist K, Gough PJ, Bertin J, Hartmann BM, Sealfon SC, Kaiser WJ, Mocarski ES, Lopez CB, Thomas PG, Oberst A, Green DR, Balachandran S. 2016. RIPK3 activates parallel pathways of MLKL-driven necroptosis and FADD-mediated apoptosis to protect against influenza A virus. Cell Host Microbe 20:13–24. https://doi.org/10.1016/j.chom.2016.05.011.
17. Zhang T, Yin C, Boyd DF, Quarato G, Ingram JP, Shubina M, Ragan KB, Ishizuka T, Crawford JC, Tummers B, Rodriguez DA, Xue J, Peri S, Kaiser WJ, Lopez CB, Xu Y, Upton JW, Thomas PG, Green DR, Balachandran S. 2020. Influenza virus Z-RNAs induce ZBP1-mediated necroptosis. Cell 180:1115–1129. https://doi.org/10.1016/j.cell.2020.02.050.
18. Fenner F. 1947a. Studies in infectious ectromelia of mice; natural transmission: the portal of entry of the virus. Aust J Exp Biol Med 25:275–282. https://doi.org/10.1038/icb.1947.39.
19. Schell K. 1960. Studies on the innate resistance of mice to infection with mousepox. Aust J Exp Biol Med Sci 38:271–288. https://doi.org/10.1038/icb.1960.29.
20. Ferez M, Knudson CJ, Lev A, Wong EB, Alves-Peixoto P, Tang L, Stotesbury C, Sigal LJ. 2021. Viral infection modulates Qa-1b in infected and bystander cells to properly direct NK cell killing. J Exp Med 218. https://doi.org/10.1084/jem.20201782.

21. Wong EB, Montoya B, Ferez M, Stotesbury C, Sigal LJ. 2019. Resistance to ectromelia virus infection requires cGAS in bone marrow-derived cells which can be bypassed with cGAMP therapy. PLoS Pathog 15:e1008239. https://doi.org/10.1371/journal.ppat.1008239.
22. Rubio D, Xu RH, Remakus S, Krouse TE, Truckenmiller ME, Thapa RJ, Balachandran S, Alcami A, Norbury CC, Sigal LJ. 2013. Crosstalk between the type 1 interferon and nuclear factor kappa B pathways confers resistance to a lethal virus infection. Cell Host Microbe 13:701–710. https://doi.org/10.1016/j.chom.2013.04.015.
23. Wong E, Montoya B, Stotesbury C, Ferez M, Xu RH, Sigal LJ. 2019. Langerhans cells orchestrate the protective antiviral innate immune response in the lymph node. Cell Rep 29:3047–3059. https://doi.org/10.1016/j.celrep.2019.10.118.
24. Xu RH, Cohen M, Tang Y, Lazear E, Whitbeck JC, Eisenberg RJ, Cohen GH, Sigal LJ. 2008. The orthopoxvirus type I IFN binding protein is essential for virulence and an effective target for vaccination. J Exp Med 205:981–992. https://doi.org/10.1084/jem.20071854.
25. Melo-Silva CR, Alves-Peixoto P, Heath N, Tang L, Montoya B, Knudson CJ, Stotesbury C, Ferez M, Wong E, Sigal LJ. 2021. Resistance to lethal ectromelia virus infection requires Type I interferon receptor in natural killer cells and monocytes but not in adaptive immune or parenchymal cells. PLoS Pathog 17:e1009593. https://doi.org/10.1371/journal.ppat.1009593.
26. Sigal LJ. 2016. The pathogenesis and immunobiology of mousepox. Adv Immunol 129:251–276. https://doi.org/10.1016/bs.ai.2015.10.001.
27. Xu RH, Wong EB, Rubio D, Roscoe F, Ma X, Nair S, Remakus S, Schwendener R, John S, Shlomchik M, Sigal LJ. 2015. Sequential activation of two pathogen-sensing pathways required for type I interferon expression and resistance to an acute DNA virus infection. Immunity 43:1148–1159. https://doi.org/10.1016/j.immuni.2015.11.015.
28. Rock KL, Reits E, Neefjes J. 2016. Present yourself! By MHC class I and MHC class II molecules. Trends Immunol 37:724–737. https://doi.org/10.1016/j.it.2016.08.010.
29. Remakus S, Rubio D, Ma X, Sette A, Sigal LJ. 2012. Memory CD8+ T cells specific for a single immunodominant or subdominant determinant induced by peptide-dendritic cell immunization protect from an acute lethal viral disease. J Virol 86:9748–9759. https://doi.org/10.1128/JVI.00981-12.
30. Fang M, Sigal LJ. 2005. Antibodies and CD8+ T cells are complementary and essential for natural resistance to a highly lethal cytopathic virus. J Immunol 175:6829–6836. https://doi.org/10.4049/jimmunol.175.10.6829.
31. Fang M, Lanier LL, Sigal LJ. 2008. A role for NKG2D in NK cell-mediated resistance to poxvirus disease. PLoS Pathog 4:e30. https://doi.org/10.1371/journal.ppat.0040030.
32. Balachandran S, Mocarski ES. 2021. Viral Z-RNA triggers ZBP1-dependent cell death. Curr Opin Virol 51:134–140. https://doi.org/10.1016/j.coviro.2021.10.004.
33. Remakus S, Rubio D, Lev A, Ma X, Fang M, Xu RH, Sigal LJ. 2013. Memory CD8(+) T cells can outsource IFN-gamma production but not cytolytic killing for antiviral protection. Cell Host Microbe 13:546–557. https://doi.org/10.1016/j.chom.2013.04.004.
34. Porgador A, Yewdell JW, Deng Y, Bennink JR, Germain RN. 1997. Localization, quantitation, and in situ detection of specific peptide-MHC class I complexes using a monoclonal antibody. Immunity 6:715–726. https://doi.org/10.1016/S1074-7613(00)80447-1.
35. Fang M, Sigal LJ. 2006. Direct CD28 costimulation is required for CD8+ T cell-mediated resistance to an acute viral disease in a natural host. J Immunol 177:8027–8036. https://doi.org/10.4049/jimmunol.177.11.8027.
36. Omoto S, Guo H, Talekar GR, Roback L, Kaiser WJ, Mocarski ES. 2015. Suppression of RIP3-dependent necroptosis by human cytomegalovirus. J Biol Chem 290:11635–11648. https://doi.org/10.1074/jbc.M115.646042.
37. Daley-Bauer LP, Roback L, Crosby LN, McCormick AL, Feng Y, Kaiser WJ, Mocarski ES. 2017. Mouse cytomegalovirus M36 and M45 death suppressors cooperate to prevent inflammation resulting from antiviral programmed cell death pathways. Proc Natl Acad Sci U S A 114:E2786–E2795. https://doi.org/10.1073/pnas.1616829114.
38. Liu Z, Nailwal H, Rector J, Rahman MM, Sam R, McFadden G, Chan FK. 2021. A class of viral inducer of degradation of the necroptosis adaptor RIPK3 regulates virus-induced inflammation. Immunity 54:247–258. https://doi.org/10.1016/j.immuni.2020.11.020.
39. Nailwal H, Chan FK. 2019. Necroptosis in anti-viral inflammation. Cell Death Differ 26:4–13. https://doi.org/10.1038/s41418-018-0172-x.
40. Hernaez B, Alonso G, Georgana I, El-Jesr M, Martin R, Shair KHY, Fischer C, Sauer S, Maluquer de Motes C, Alcami A. 2020. Viral cGAMP nuclease reveals the essential role of DNA sensing in protection against acute lethal virus infection. Sci Adv 6. https://doi.org/10.1126/sciadv.abb4565.
41. Samuelsson C, Hausmann J, Lauterbach H, Schmidt M, Akira S, Wagner H, Chaplin P, Suter M, O'Keeffe M, Hochrein H. 2008. Survival of lethal poxvirus infection in mice depends on TLR9, and therapeutic vaccination provides protection. J Clin Invest 118:1776–1784. https://doi.org/10.1172/JCI33940.
42. Hernaez B, Alonso-Lobo JM, Montanuy I, Fischer C, Sauer S, Sigal L, Sevilla N, Alcami A. 2018. A virus-encoded type I interferon decoy receptor enables evasion of host immunity through cell-surface binding. Nat Commun 9:5440. https://doi.org/10.1038/s41467-018-07772-z.
43. Mavian C, Lopez-Bueno A, Bryant NA, Seeger K, Quail MA, Harris D, Barrell B, Alcami A. 2014. The genome sequence of ectromelia virus Naval and Cornell isolates from outbreaks in North America. Virology 462–463:218–226. https://doi.org/10.1016/j.virol.2014.06.010.
44. Mohamed MR, Rahman MM, Rice A, Moyer RW, Werden SJ, McFadden G. 2009. Cowpox virus expresses a novel ankyrin repeat NF-kappaB inhibitor that controls inflammatory cell influx into virus-infected tissues and is critical for virus pathogenesis. J Virol 83:9223–9236. https://doi.org/10.1128/JVI.00861-09.
45. Mohamed MR, Rahman MM, Lanchbury JS, Shattuck D, Neff C, Dufford M, van Buuren N, Fagan K, Barry M, Smith S, Damon I, McFadden G. 2009. Proteomic screening of variola virus reveals a unique NF-kappaB inhibitor that is highly conserved among pathogenic orthopoxviruses. Proc Natl Acad Sci U S A 106:9045–9050. https://doi.org/10.1073/pnas.0900452106.
46. Blanden RV. 1970. Mechanisms of recovery from a generalized viral infection: mousepox. J Exp Med 132:19.
47. Hanggi K, Vasilikos L, Valls AF, Yerbes R, Knop J, Spilgies LM, Rieck K, Misra T, Bertin J, Gough PJ, Schmidt T, de Almodovar CR, Wong WW. 2017. RIPK1/RIPK3 promotes vascular permeability to allow tumor cell extravasation independent of its necroptotic function. Cell Death Dis 8:e2588. https://doi.org/10.1038/cddis.2017.20.
48. Fang M, Roscoe F, Sigal LJ. 2010. Age-dependent susceptibility to a viral disease due to decreased natural killer cell numbers and trafficking. J Exp Med 207:2369–2381. https://doi.org/10.1084/jem.20100282.
49. Fang M, Siciliano NA, Hersperger AR, Roscoe F, Hu A, Ma X, Shamsedeen AR, Eisenlohr LC, Sigal LJ. 2012. Perforin-dependent CD4+ T-cell cytotoxicity contributes to control a murine poxvirus infection. Proc Natl Acad Sci U S A 109:9983–9988. https://doi.org/10.1073/pnas.1202143109.